Electronic Supplementary Material (ESI) for Journal of Materials Chemistry A.
This journal is © The Royal Society of Chemistry 2020

Supporting Information

Identifying dual functions of rGO in a $BiVO_4$/rGO/NiFe-layered double hydroxide photoanode for efficient photoelectrochemical water splitting

Hua Chen,[ab†] Songcan Wang,[bc†] Jianzhong Wu,[a] Xiacong Zhang,[d] Jia Zhang,[a] Miaoqiang Lyu,[b] Bin Luo,[b] Guangren Qian,*[a] and Lianzhou Wang*[b]

[a] School of Environmental and Chemical Engineering, Shanghai University, No. 333 Nanchen Rd., Shanghai 200444, P. R. China.

[b] Nanomaterials Centre, Australian Institute for Bioengineering and Nanotechnology and School of Chemical Engineering, The University of Queensland, Brisbane, Queensland 4072, Australia.

[c] Frontiers Science Center for Flexible Electronics (FSCFE), Shaanxi Institute of Flexible Electronics (SIFE) & Shaanxi Institute of Biomedical Materials and Engineering (SIBME), Northwestern Polytechnical University (NPU), 127 West Youyi Road, Xi'an 710072, China.

[d] Department of Polymer Materials, College of Materials Science and Engineering, Shanghai University, No. 333 Nanchen Rd., Shanghai 200444, P. R. China.

* Corresponding authors: grqian@shu.edu.cn (G. Qian); l.wang@uq.edu.au (L. Wang)

† These authors contributed equally to this work.

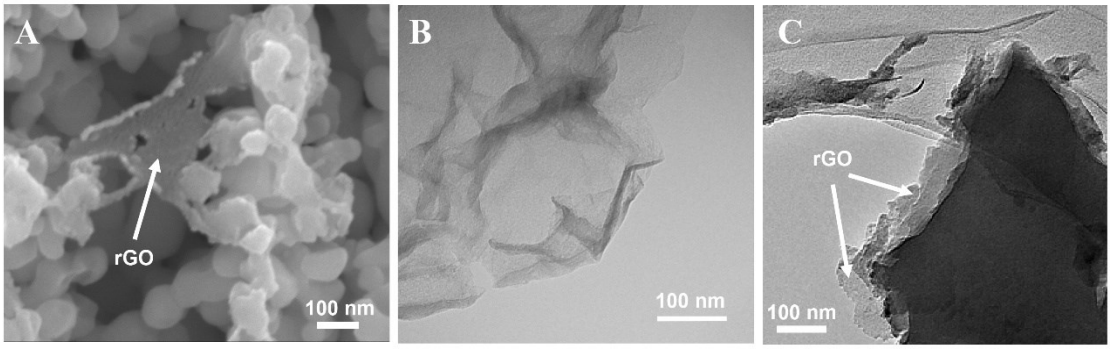

Fig. S1 (A) High resolution SEM image of $BiVO_4$/rGO. TEM images of (B) rGO and (C) $BiVO_4$/rGO.

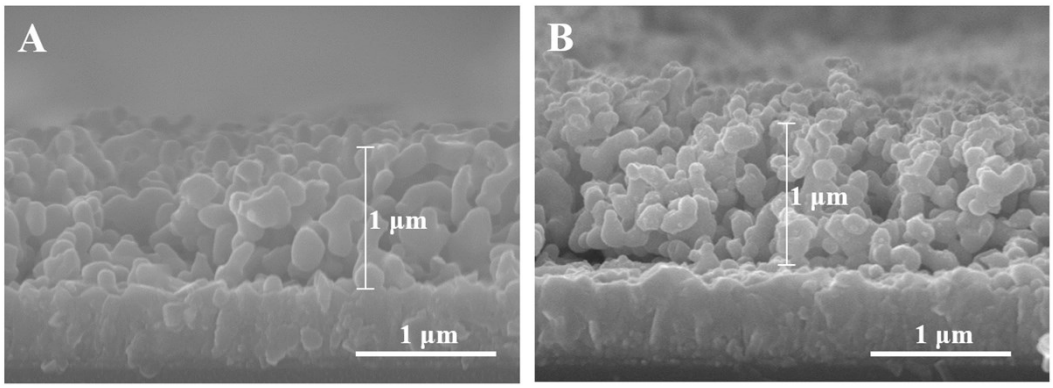

Fig. S2 SEM cross-section of (A) $BiVO_4$, and (B) $BiVO_4$/rGO/NiFe-LDH.

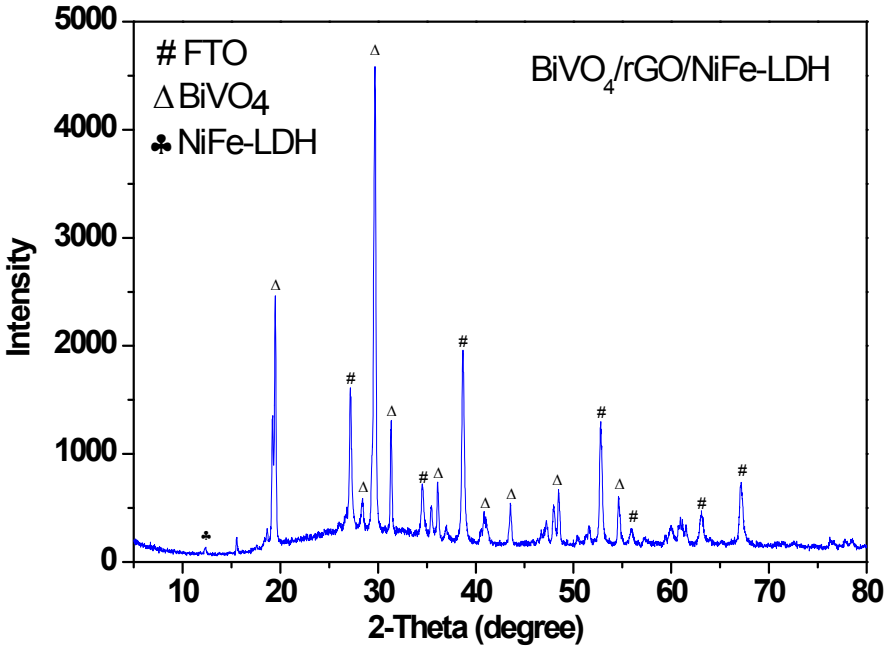

Fig. S3 XRD pattern of $BiVO_4$/rGO/NiFe-LDH.

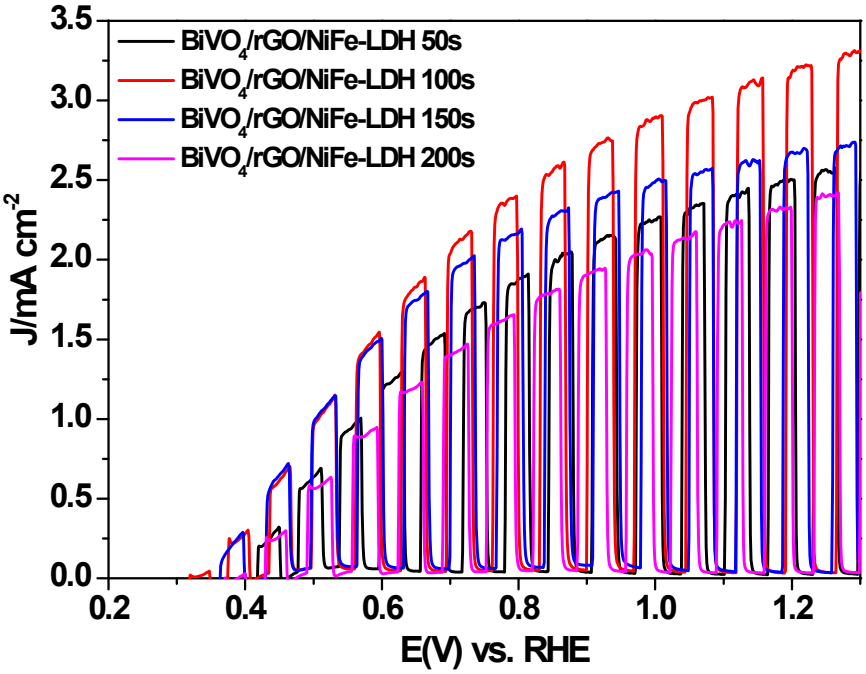

Fig. S4 LSV curves of $BiVO_4$/rGO/NiFe-LDH with various LDH deposition time.

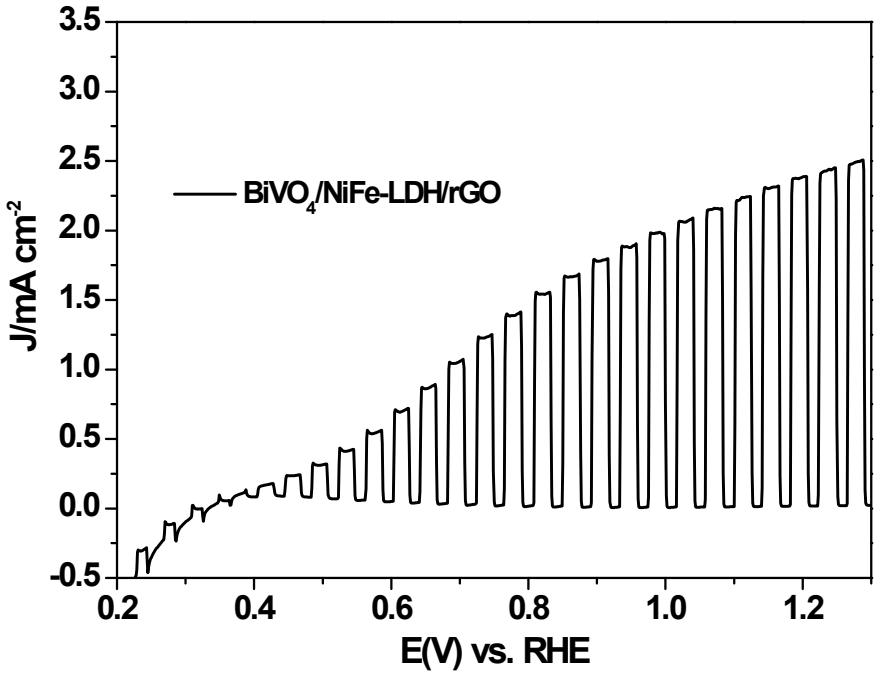

Fig. S5 LSV curves $BiVO_4$/NiFe-LDH/rGO.

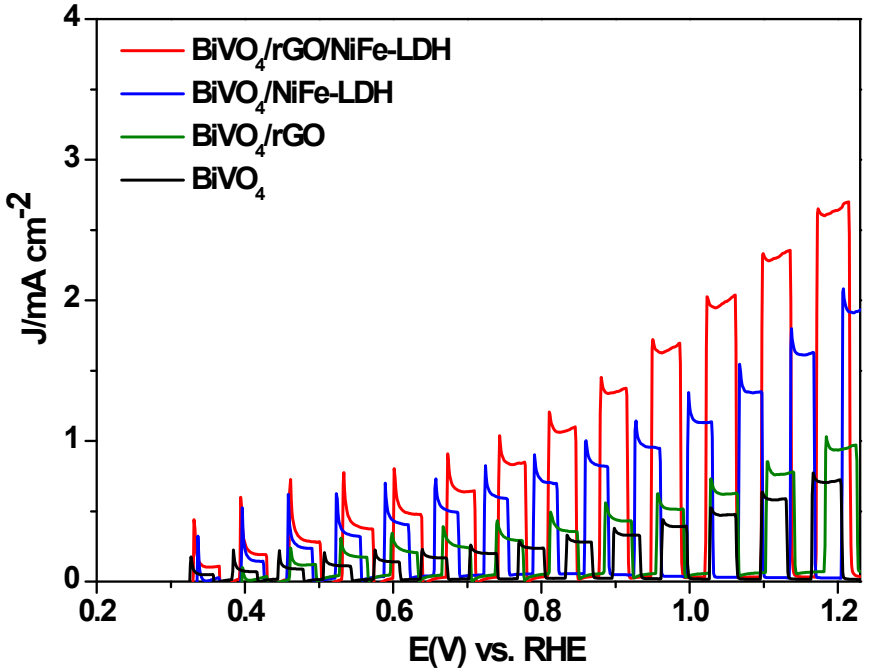

Fig. S6 LSV curves of the as-prepared photoanodes in 1 M $KHPO_4$ electrolyte (pH=7).

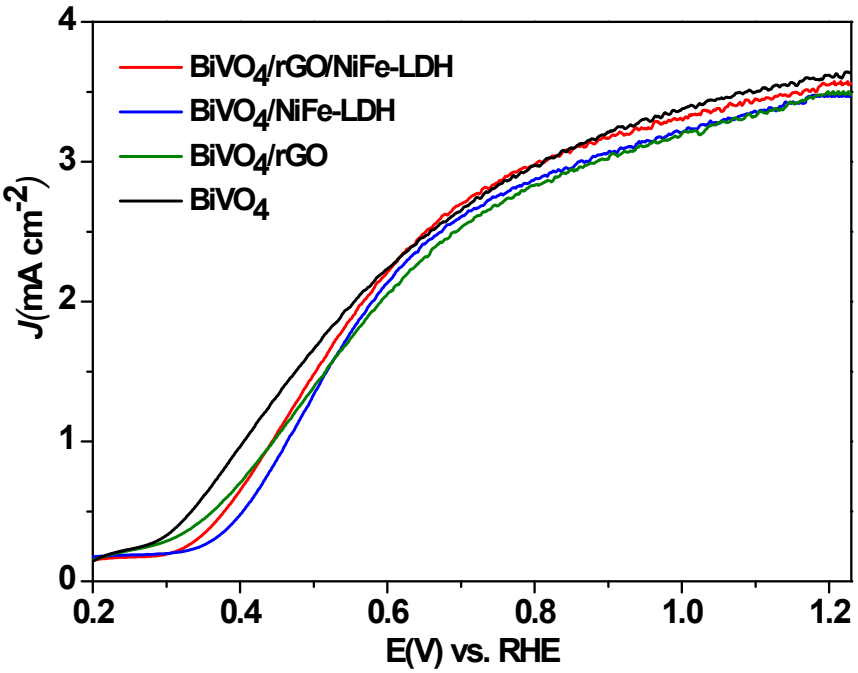

Fig. S7 LSV curves of the as-prepared photoanodes in the presence of 0.2 M Na_2SO_3.

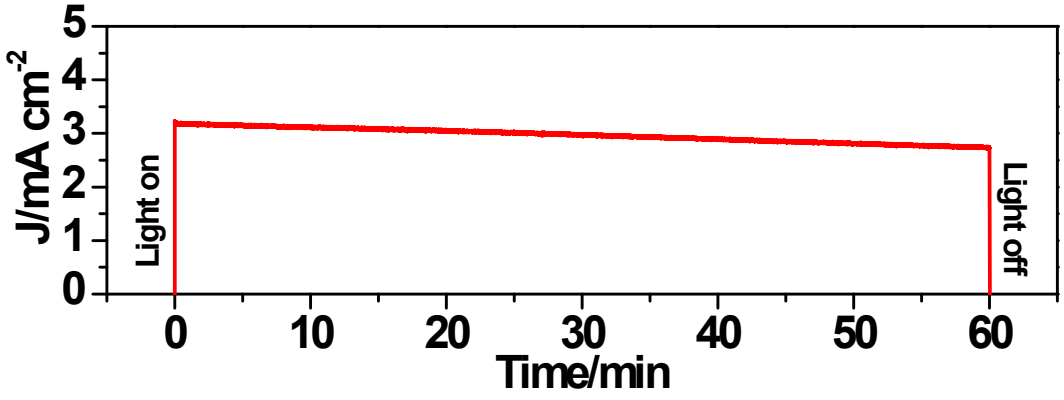

Fig. S8 Stability measurement of $BiVO_4$/rGO/NiFe-LDH under consecutive AM 1.5 G illumination at 1.23 V *vs.* RHE.

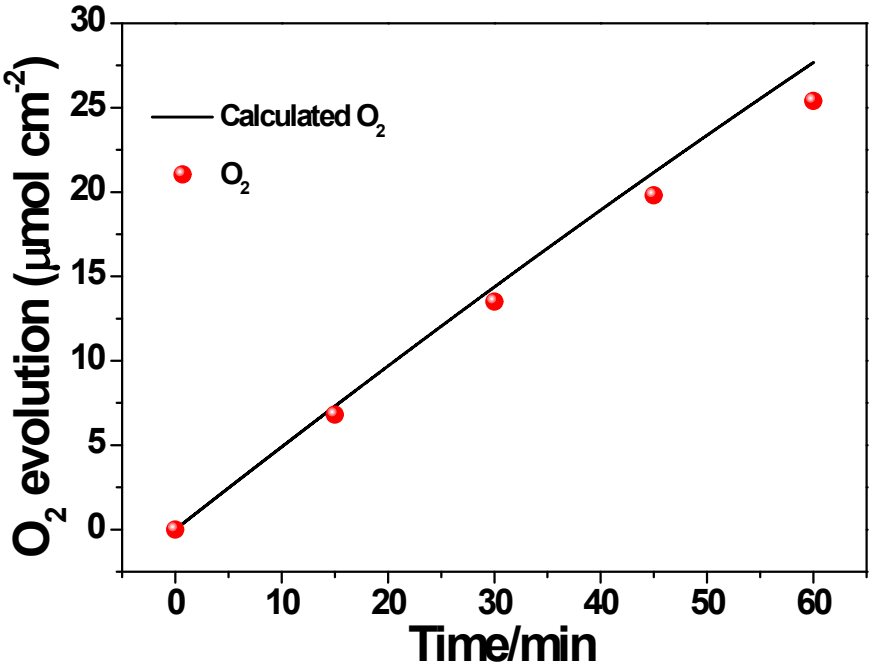

Fig. S9 O_2 evolution of $BiVO_4$/rGO/NiFe-LDH under consecutive AM 1.5 G illumination at 1.23 V *vs.* RHE.

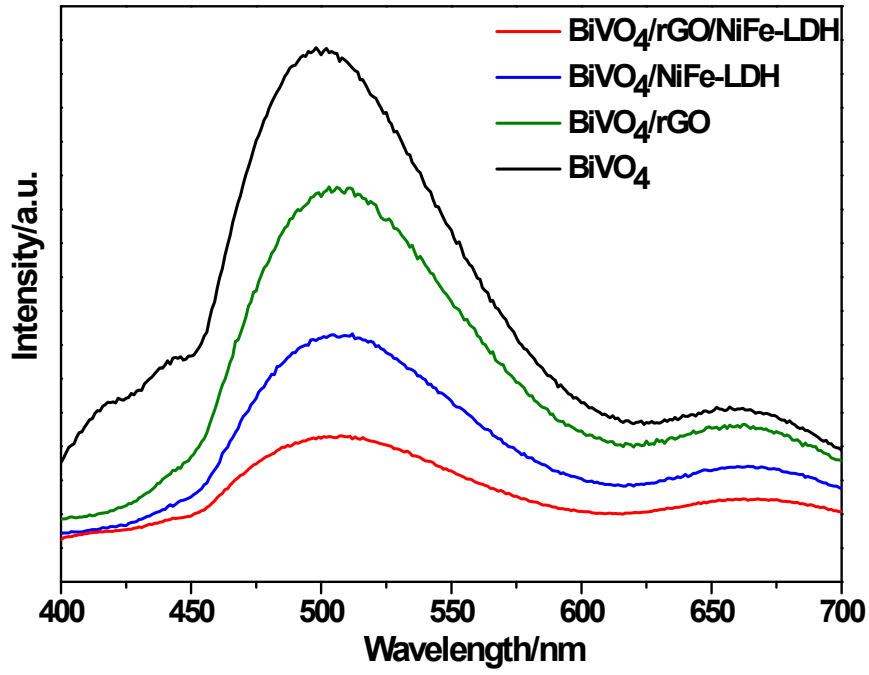

Fig. S10 PL spectra of $BiVO_4$, $BiVO_4$/rGO, $BiVO_4$/NiFe-LDH, and $BiVO_4$/rGO/NiFe-LDH.

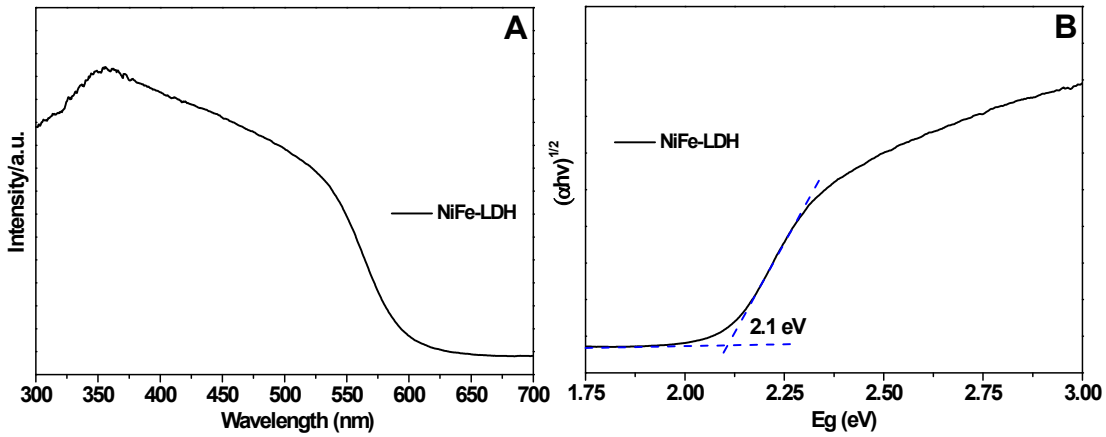

Fig. S11 (A) UV-Vis diffuse reflectance spectra, and (B) Corresponding plot of transformed Kubelka-Munk function versus the energy of the light of NiFe-LDH.

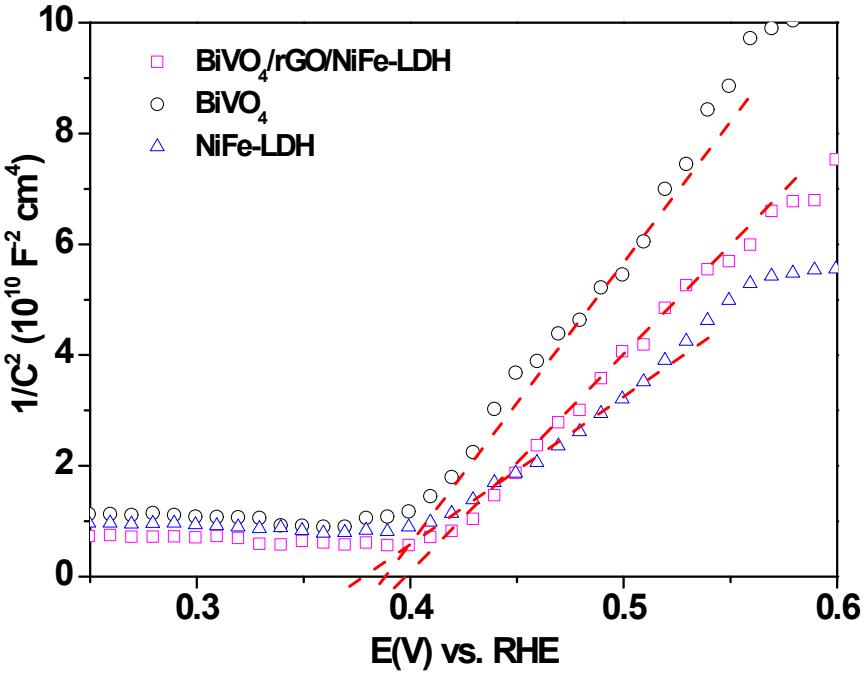

Fig. S12 Mott-Schottky plots of NiFe-LDH, pristine $BiVO_4$ and $BiVO_4$/rGO/NiFe-LDH measured in 1 kHz at room temperature in the dark.

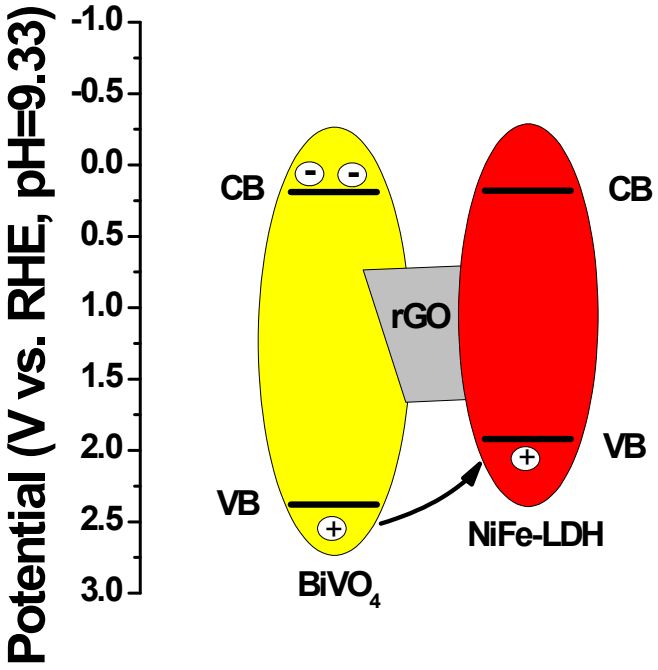

Fig. S13 Band alignment and mechanism of charge separation for the $BiVO_4$/rGO/NiFe-LDH photoanode.

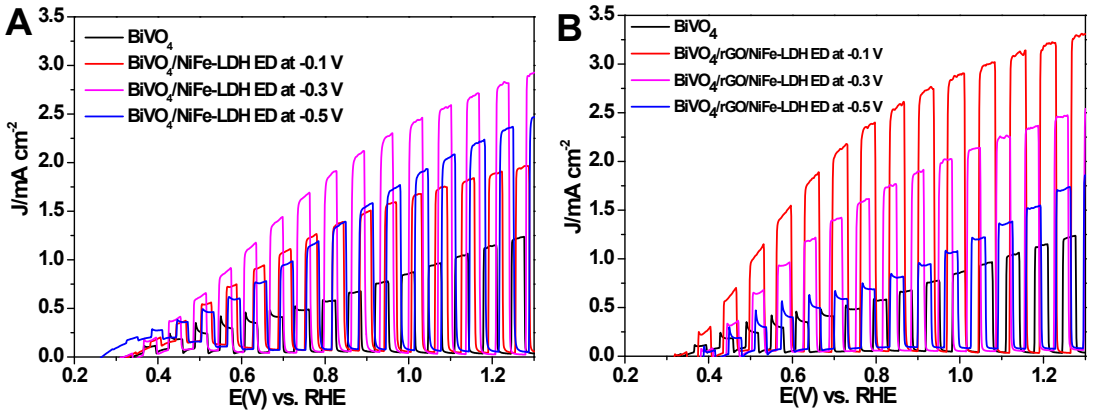

Fig. S14 LSV curves of (A) Pristine $BiVO_4$ and (B) $BiVO_4$/rGO with various LDH deposition potential (time for 100 s).

Table S1 The fitted results of EIS data using the equivalent circuit in Fig. 5D.

Samples	R_s/Ω	R_{ct}/Ω
$BiVO_4$	26.2 ± 0.2	540.0 ± 4.5
$BiVO_4$/NiFe-LDH	21.0 ± 0.1	403.0 ± 3.5
$BiVO_4$/rGO/NiFe-LDH	28.0 ± 0.1	248.0 ± 2.4